

Electronic Supplementary Information

**A ratiometric nanoarchitecture for the
simultaneous detection of pH and halide
ions using UV plasmon-enhanced
fluorescence**

Jérémie Asselin, Marie-Pier Lambert, Nicolas Fontaine, Denis Boudreau*

Département de chimie et Centre d'optique photonique et laser (COPL), Université Laval,
Québec (QC), Canada G1V 0A6

* Corresp. author: denis.boudreau@chm.ulaval.ca. 418-656-3287 (ph.), 418-656-7916 (fax).

1. MATERIAL AND METHODS

Chemicals and Reagents. Sodium citrate dibasic sesquihydrate (99%, ACS grade), diethylene glycol (99%), triethylamine ($\geq 99.5\%$), (3-aminopropyl) triethoxysilane (APTES; $\geq 98\%$), ammonium hydroxide solution (28-30% wt NH_3), dimethylamine (DMA; 40% wt solution in water), sodium borohydride (99.99%), Rhodamine B isothiocyanate (RBITC, mixed isomers), Rhodamine B ($\sim 95\%$), fluorescein 5(6)-isothiocyanate (FITC; 90%) and 6-methoxyquinoline (98%) were purchased from Sigma-Aldrich. Tetraethoxysilane (TEOS; 99.9%) and potassium bromide (ACS grade, $>99\%$) were obtained from Alfa Aesar. Indium (III) chloride tetrahydrate (99.9%) was obtained from Strem Chemicals, potassium chloride (ACS grade, 99.0%) from BDH Inc., anhydrous *N,N*-dimethylformamide (DMF; 99.8%) from EMD Chemicals, 6-methoxy-*N*-ethylquinolium iodide from Molecular Probes and 11-bromoundecyltriethoxysilane ($\geq 95\%$) from SiKÉMIA. Potassium iodide (ACS grade), potassium phosphate monobasic ($>99\%$) and dibasic ($>98\%$) were purchased from Anachemia. Unless otherwise stated, nanopure water (18 M Ω) and anhydrous ethanol (Commercial Alcohols, Brampton, ON, Canada) were used in all experiments, and chemical reagents were used without further purification. All glassware was conditioned with hydrofluoric acid, before further cleaning with nitric acid and rinsed thoroughly with nanopure water.

Synthesis of In plasmonic cores.¹ 367 mg of indium chloride ($\text{InCl}_3 \cdot 4 \text{H}_2\text{O}$) and 245 mg of sodium citrate ($\text{Na}_2\text{Cit} \cdot 1.5 \text{H}_2\text{O}$) were added to 50 mL of diethylene glycol in a three-necked round-bottomed flask and heated to 100 °C under nitrogen atmosphere and vigorous stirring for 35 minutes. Injection of 2 mL of a 2.45 M solution of sodium borohydride allowed the formation of highly spherical nanoparticles with an average diameter of (70 \pm 20) nm. The colloidal

suspension was left to stir for 15 minutes and then cooled down to room temperature. The resulting nanoparticles were centrifuged at 12,000 RCF (15 minutes) and dispersed in 15 mL of ethanol.

Preparation of fluorescent isothiocyanates.^{2,3} The fluorescent dyes used as reference and pH sensor were commercially available Rhodamine B isothiocyanate (RBITC) and fluorescein isothiocyanate (FITC), respectively. The dyes were reacted with APTES to form RB-APS and FL-APS following a methodology previously optimized in our research group. 23 μ moles of fluorophore was dissolved (12.2 mg of RBITC, 8.8 mg of FITC) in 450 μ L of anhydrous DMF. 6.4 μ L of APS and 6.4 μ L of triethylamine were added and the resulting mixture was left to react in the dark at room temperature for 3 hours. The APS-modified rhodamine B or fluorescein solution was diluted to 50 mL with ethanol and stored in the dark at -20 °C until use (within one week after their preparation).

Preparation of silanized methoxyquinolinium.⁴ Preparation of the silane-modified 6-methoxyquinolinium dye was taken from the work of Baù et al. 80 mg of 6-methoxyquinoline was solubilized in 200 mg of 11-bromoundecyltriethoxysilane and the mixture was heated to 95°C under nitrogen flow and vigorous agitation for 20 hours. The final solution was diluted to 50 mL in ethanol and kept in the dark at -20 °C.

Preparation of multishell nanoarchitectures. The condensation of silica shells on metallic colloids was performed using an ammonia-free synthesis route adapted from the literature (**Fig. 1**).^{2,5} In a 50-mL polypropylene conical tube, 20 mL of ethanol, 0.5 mL of a 9 mM TEOS solution, 1.0 mL of In NPs suspension, 0.25 mL of DMA 40% wt and 2.0 mL of water were mixed vigorously for 15 minutes, before the addition of 75 μ L of RB-APS solution. In@SiO₂+RB NPs

(abbreviated In@(RB)) were left to react for 20-24 hours, centrifuged three times at 8,000 RCF (10 minutes) and then dispersed in 30 mL of ethanol.

For the second shell, 12.5 mL of In@(RB) dispersion was diluted with 13.4 mL of 95% ethanol. A precise volume (0.2 to 5.0 mL) of a 9 mM TEOS solution was added, depending on the desired spacer thickness (1 to 40 nm, **Fig. S2**), before the addition of 0.3 mL of DMA 40% wt and 0.25 mL of FL-APS moieties. After 20-24 h of condensation, the resulting In@SiO₂+RB@SiO₂+FL core-shell NPs (abbreviated In@(RB)@(FL)) were centrifuged three times at 8,000 RCF (10 min) and dispersed in 10 mL ethanol. Finally, the silane-modified 6-methoxyquinolinium was covalently bound to the outer surface of In@(RB)@(FL) by condensation with ammonia as catalyst. 20 μL of MQ-silane precursor and 150 μL of 30% wt ammonia aqueous solution were added to the previous dispersion of core-multishell colloids in ethanol and allowed to react for 4 hours under vigorous stirring at room temperature. The resulting In@SiO₂+RB@SiO₂+FL@MQ nanostructures (abbreviated In@(RB)@(FL)@MQ) were centrifuged three times at 8,000 RCF (10 min) and finally dispersed in 10 mL of ethanol.

Preparation of pH buffers and halide solutions. The phosphate buffers were prepared with different ratios of KH₂PO₄ and K₂HPO₄ at 0.1 M to modulate pH, with additions of KCl, KBr and KCl to modulate halide ion concentrations. The choice of these potassium salts in our experiments was made to introduce only one cationic species and to limit its reactivity toward our core-multishell In@SiO₂ architectures.

Characterization. Nanoparticles were characterized by UV-visible spectrophotometry (Cary 50, Agilent Technologies) and transmission electronic microscopy (TEM, Tecnai G2 Spirit, FEI). Fluorescent core-multishell nanoparticles were characterized by spectrofluorimetry (Fluorolog 3, Jobin-Yvon Horiba), Zeta-potential measurements (Nano ZS Zetasizer, Malvern Instruments) and

time-resolved fluorescence decay measurements (custom-made system using a 308 nm XeCl excimer laser source). Fluorescence decay curves were fitted with a single-exponential model with reconvolution of the instrumental response function (FluoFit data analysis software, PicoQuant GmbH).

B. METHODOLOGIES

Measurement of silica shells. The thickness of the silica shells condensed around indium cores was measured by using transmission electronic micrographs processed with the iSOLUTION software (IMT; Cicero, NY). Briefly, the thickness value corresponds to the length of a radial line traced through the dielectric shell, which can be distinguished by a change in contrast. The average values and standard deviations presented in this work were measured with three radial lines for every colloids, for over 150 particles in each sample.

Evaluation of MQ enhancement factors. The improvement in fluorescence signal was estimated with the condensation of thick silica spacer shells, where MQ is positioned outside of the plasmonic range of In cores. The ratiometric I_{MQ}/I_{RB} intensity of In@(RB)@SiO₂@MQ with 45 nm spacers ($N = 3$) was used as F_0 value to calculate enhancement factors (F/F_0).

Application of ratiometry in In@(RB)@(FL)@MQ. In order to minimize the influence of energy transfer mechanisms in our concentric multi-elementary nanosensors, spectrofluorimetric experiments were achieved by successive excitation of each fluorophores and integration of the intensity values at maximal wavelengths of emission. Instrumental parameters are presented in Table S1.

Table S1.

wavelengths used	Fluorescence		
	Fluorophore	Excitation (nm)	Emission (nm)
	MQ	340	430-470
	FL (acidic)	440	510-550
	FL (basic)	490	510-550
	RB	540	575-615

for

In@(RB)@(FL)@MQ

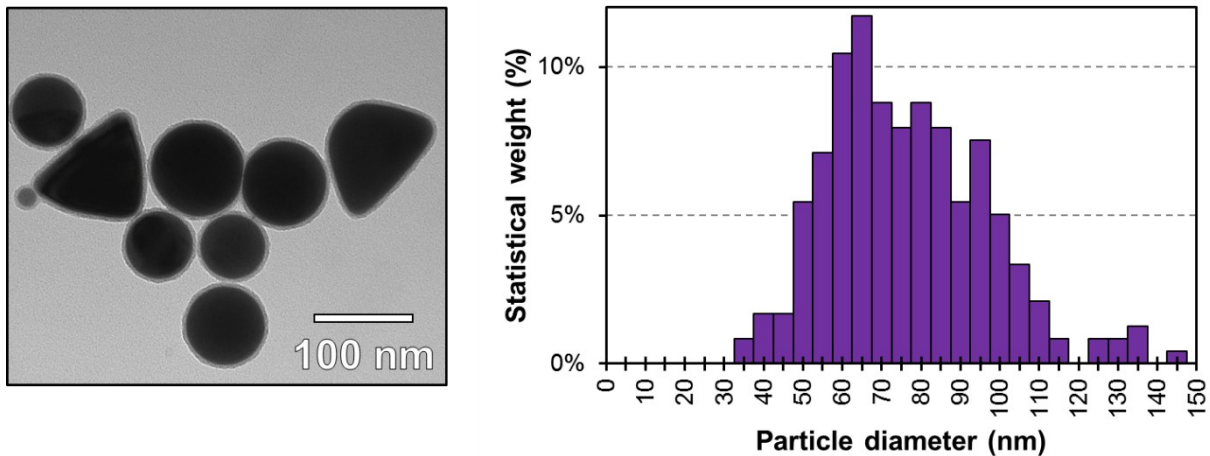


Figure S1. Transmission electronic micrograph of In@(RB) NPs (indium cores: 70 ± 20 nm, silica shell: 5.1 ± 0.3 nm) and corresponding size distribution histogram for the In cores.

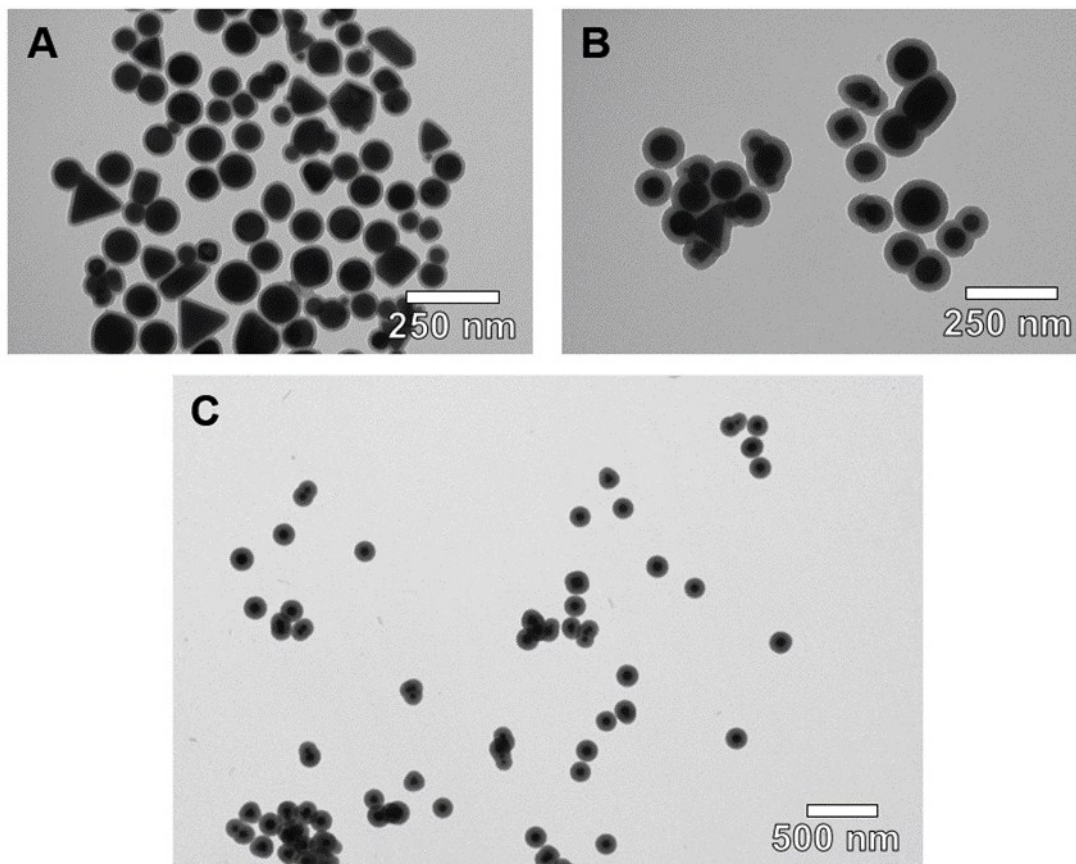


Figure S2. Transmission electronic micrograph of $\text{In}@\text{(RB)}@\text{(FL)}@\text{MQ}$ with different silica spacer thickness (A: 10.8 ± 0.9 nm, B: 20 ± 1 nm, C: 41 ± 1 nm).

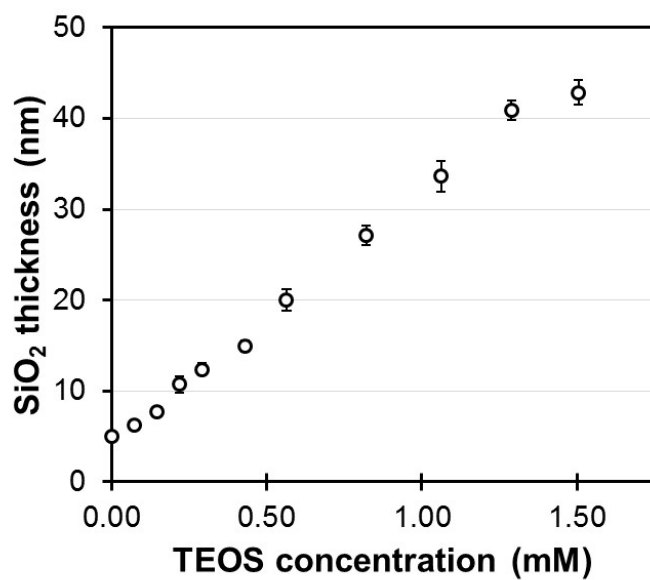


Figure S3. Modulation of the second silica shell through variation in TEOS concentration during the Stober reaction.

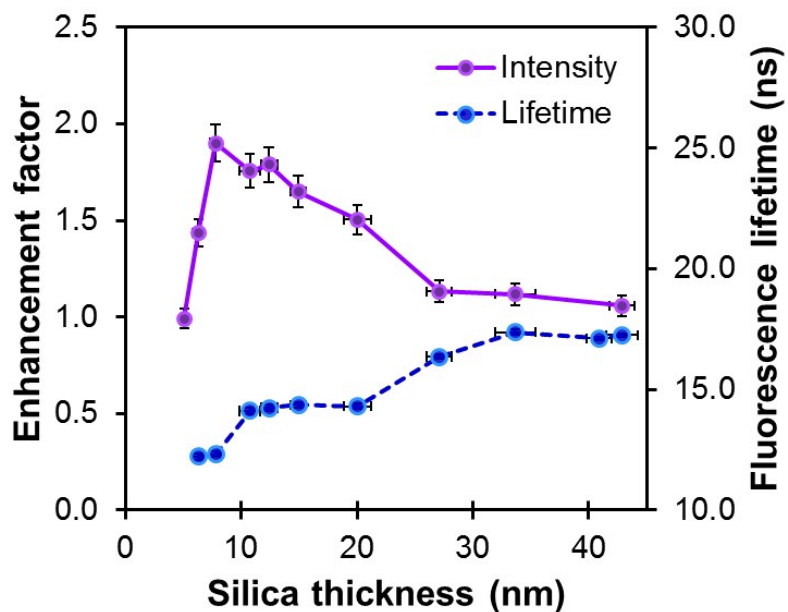


Figure S4. Values of fluorescence intensity enhancement ($\lambda_{ex} = 340 \text{ nm}$, $\lambda_{em} = 440 \text{ nm}$) and lifetime ($\lambda_{ex} = 308 \text{ nm}$) for MQ in $\text{In}@\text{(RB)}@\text{SiO}_2@\text{MQ}$ architectures as a function of spacer thickness.

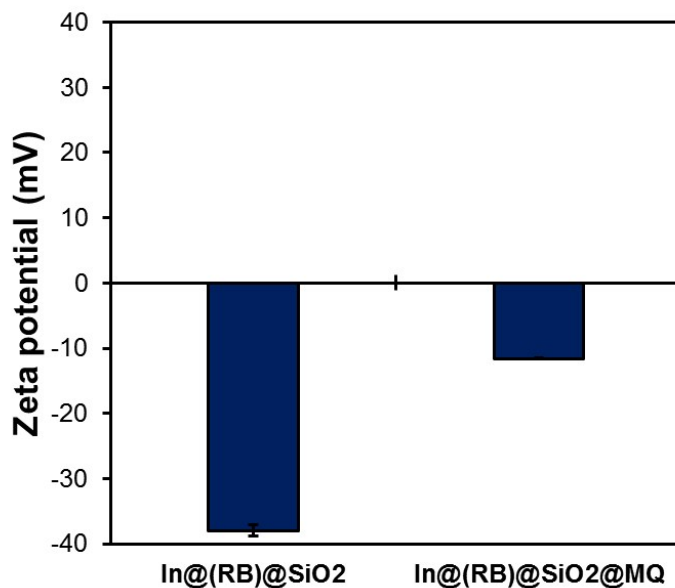


Figure S5. Zeta potential values for $\text{In}@\text{(RB)}@\text{SiO}_2$ architectures in nanopure water before and after the binding reaction of silanized MQ.

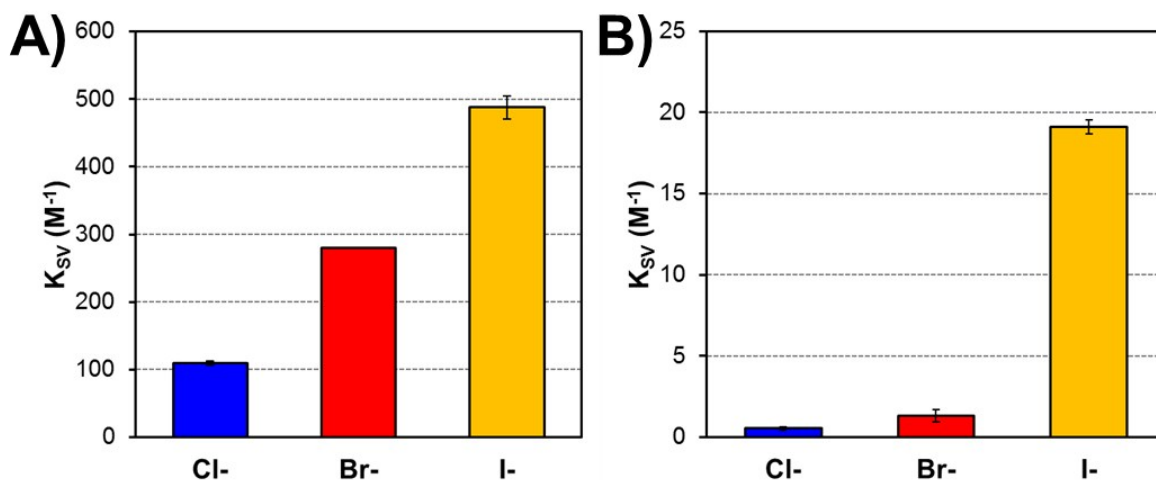


Figure S6. Stern-Volmer constant values for molecular MQ (A) and RB (B) in the presence of chloride (blue), bromide (red) and iodide (yellow). The concentration was 1×10^{-6} M for MQ and RB.

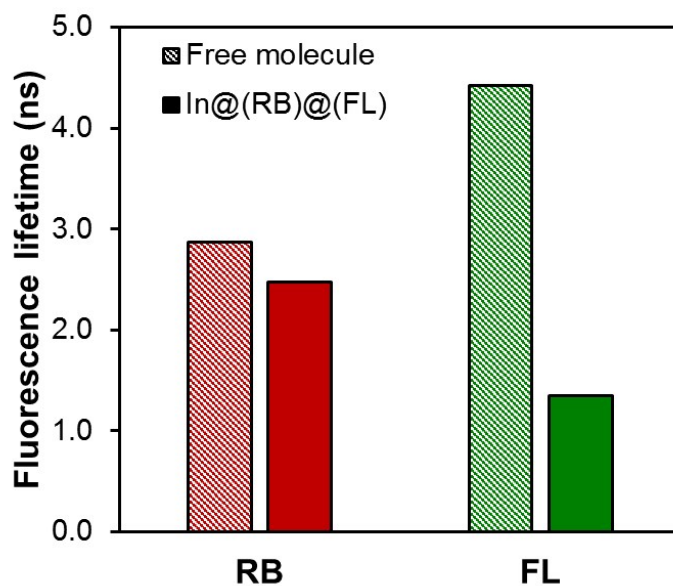


Figure S7. Excited state lifetime values measured for Rhodamine B (RB) and fluorescein (FL) in In@(RB)@(FL) and in solution ($\lambda_{ex}=488$ nm). The concentration was 1×10^{-6} M for RB and FL. Fluorophores were excited at 488 nm and fluorescence emission was measured at 580 nm (RB) and 520 nm (FL).

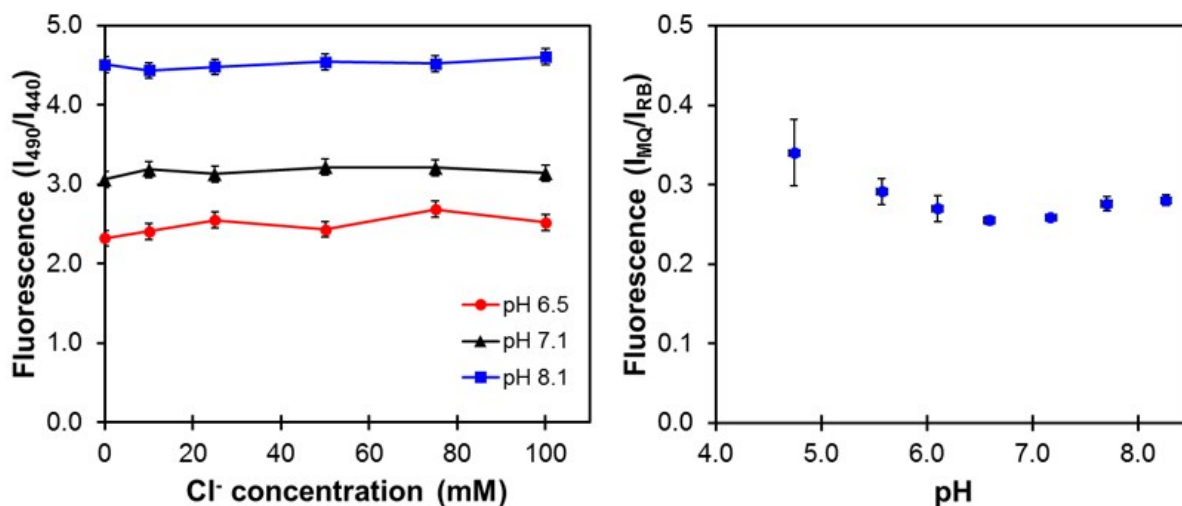


Figure S8. A) Stability range for pH-sensitive ratiometry of $In@(RB)@(FL)@MQ$ (20-nm) in three buffer compositions with regards to chloride concentration. B) Halide ion-sensitive fluorescence ratiometry (MQ/RB) with regards to pH.

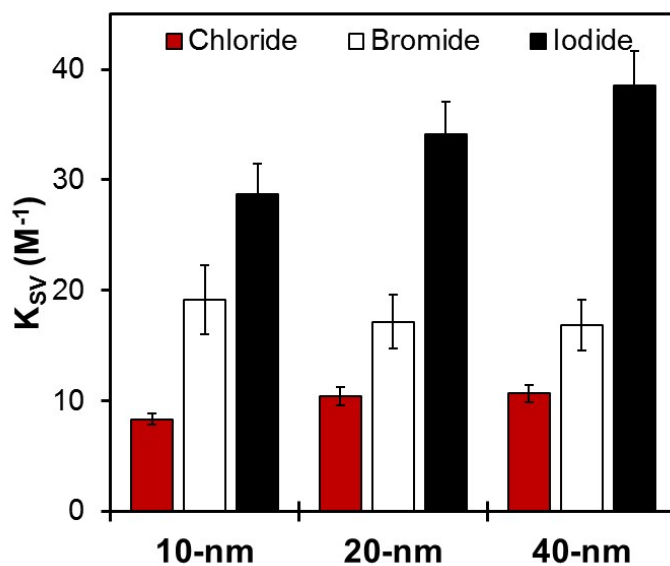


Figure S9. Stern-Volmer constants for Cl^- , Br^- and I^- with different $In@(RB)@SiO_2@MQ$ colloidal architectures.

ACKNOWLEDGEMENTS.

This work was supported by the Natural Sciences and Engineering Research Council of Canada, the “Fonds de la Recherche du Québec – Nature et Technologies” and the Canadian Foundation for Innovation. We acknowledge Mrs. Julie-Christine Lévesque and the Centre de Recherche en Infectiologie for technical assistance on the TEM imaging platform. The authors would also like to thank Félix-Antoine Lavoie and Philippe Legros for insightful discussions.

REFERENCES.

- 1 F. Magnan, J. Gagnon, F.-G. Fontaine and D. Boudreau, *Chem. Commun.*, 2013, **49**, 9299–301.
- 2 J. Asselin, P. Legros, A. Grégoire and D. Boudreau, *Plasmonics*, 2016, **11**, 1369–1376.
- 3 M. L. Viger, L. S. Live, O. D. Therrien and D. Boudreau, *Plasmonics*, 2008, **3**, 33–40.
- 4 L. Baù, F. Selvestrel, M. Arduini, I. Zamparo, C. Lodovichi and F. Mancin, *Org. Lett.*, 2012, **14**, 2984–2987.
- 5 Y. Kobayashi, H. Katakami, E. Mine, D. Nagao, M. Konno and L. M. Liz-Marzán, *J. Colloid Interface Sci.*, 2005, **283**, 392–396.